

# SUPPLEMENTARY INFORMATION

## **Seipin governs phosphatidic acid homeostasis at the inner nuclear membrane**

Anete Romanauska<sup>1,2</sup>, Edvinas Stankunas<sup>1,3,4</sup>, Maya Schuldiner<sup>5</sup> and  
Alwin Köhler<sup>1,2,3\*</sup>

<sup>1</sup>Max Perutz Labs, Vienna Biocenter Campus (VBC), Dr. Bohr-Gasse 9/3, 1030 Vienna, Austria

<sup>2</sup>University of Vienna, Dr.-Bohr-Gasse 9/3, 1030, Vienna, Austria

<sup>3</sup>Medical University of Vienna, Dr.-Bohr-Gasse 9/3, 1030, Vienna, Austria

<sup>4</sup>Vienna BioCenter PhD Program, Doctoral School of the University of Vienna and Medical University of Vienna

<sup>5</sup>Department of Molecular Genetics, Weizmann Institute of Science, Rehovot 7610001, Israel

\*Corresponding author: [alwin.koehler@maxperutzlabs.ac.at](mailto:alwin.koehler@maxperutzlabs.ac.at)

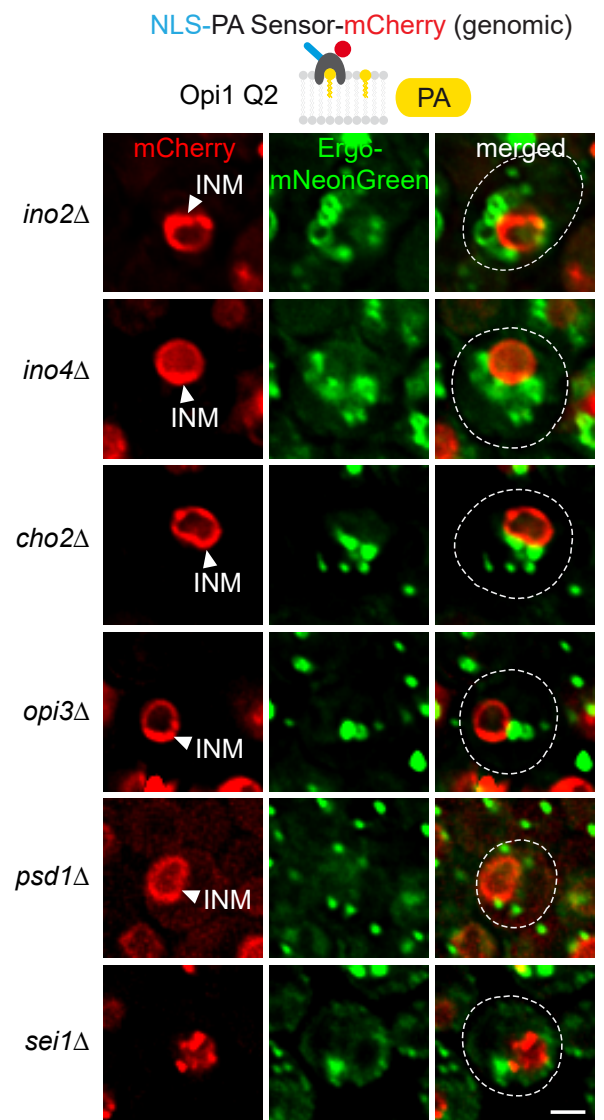
a

Biological process	Deletion library	VAL I	VAL II	PA loc.
PL biosynthesis	<i>INO2*</i>	+	+	INM/foci
PL biosynthesis	<i>INO4*</i>	+	+	INM/foci
PL biosynthesis	<i>CHO2*</i>	+	+	INM
PL biosynthesis	<i>OPI3*</i>	+	+	INM
PL biosynthesis	<i>PSD1</i>	+	+	INM
Lipid droplet formation	<i>SEI1</i>	+	+	foci
Regulator of PL metabolism	<i>SCS2</i>	-	n.d.	INM
CCR4-NOT complex subunit, regulator of mRNA stability/decay	<i>CCR4</i>	-	n.d.	foci
Mediator subunit, transcription initiation	<i>MED5</i>	+	-	foci
Casein kinase 2 subunit	<i>CKA2</i>	Not tested <sup>3</sup>	-	foci
60S ribosomal protein	<i>RPL6A<sup>1</sup></i>	-	n.d.	INM
40S ribosomal protein	<i>RPS4A</i>	-	n.d.	foci
Mitochondrial translational activator	<i>PET122</i>	-	n.d.	<sup>2</sup>
Galactokinase, galactose metabolism	<i>GAL1</i>	-	n.d.	<sup>2</sup>
Transduction of mating signal	<i>FYV5<sup>1</sup></i>	-	n.d.	foci
Regulator of <i>INO1</i>	<i>YET1</i>	-	n.d.	INM
Function unknown	<i>YGL149W</i>	-	n.d.	foci
Function unknown	<i>YNL146C-A</i>	-	n.d.	<sup>2</sup>
Function unknown	<i>YNL162W-A</i>	-	n.d.	<sup>2</sup>

b

Biological process	DAmP library	VAL I	VAL II	PA loc.
Component of the Mcm2-7 hexameric helicase complex	<i>CDC46</i>	-	n.d.	foci
Component of the RSC chromatin remodeling complex	<i>RSC8</i>	-	n.d.	foci
Nucleolar protein, ribosomal small subunit biogenesis	<i>NOP14</i>	-	n.d.	foci
40S ribosomal protein	<i>RPS20</i>	-	n.d.	foci
Nucleolar protein, ribosome biogenesis	<i>RRB1</i>	-	n.d.	foci
Function unknown	<i>YRB2</i>	-	n.d.	foci
Function unknown	<i>YIL171W</i>	-	n.d.	foci

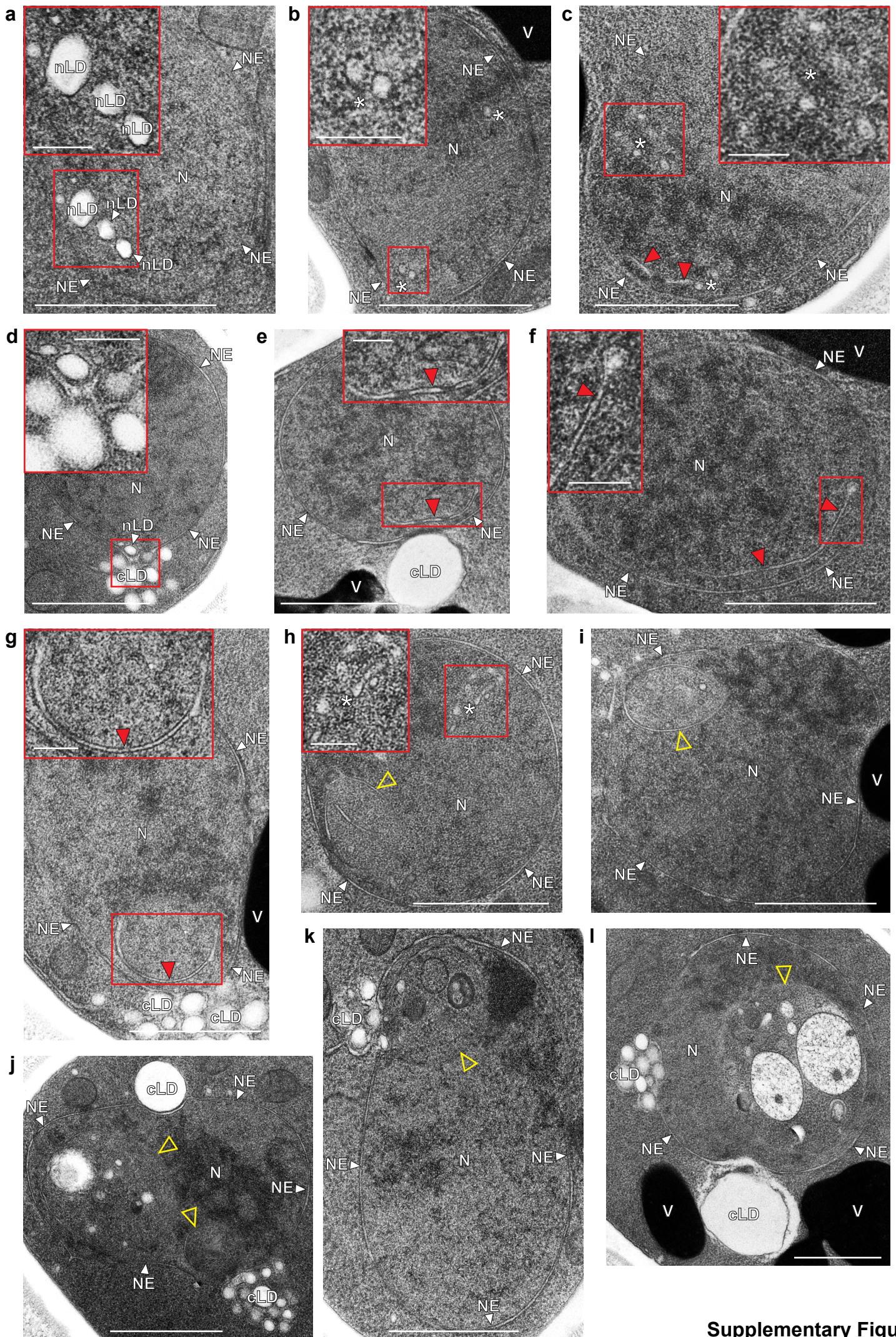
c



**Supplementary Fig. 1 | Summary of high-throughput screening of PA regulators.**

**a** Table showing deletion library hits, their biological function and result of the two-step validation (VAL I and VAL II) process, where '+' indicates a positive hit and where '-' indicates a negative hit. \* - less than 100 cells in the images; <sup>1</sup> - only one image shows prominent defects in PA sensor localization; <sup>2</sup> - varied PA sensor localization that cannot be described as foci or INM staining; <sup>3</sup> – not tested during the first validation and therefore included and tested during the second validation. Note that for the validated hits, the PA sensor localization (PA loc.) is indicated according to the final validation results. PL, phospholipid, n.d., not determined. **b** Table showing DAmP library hits, their biological function and result of the validation (VAL I and VAL II) process, where '-' indicates a negative hit. PA loc., PA sensor localization; n.d., not determined. **c** Live imaging of the validated hits expressing genomically integrated NLS-PA-mCherry sensor and *ERG6*-mNeonGreen. INM, inner nuclear membrane. Scale bar, 2  $\mu$ m.



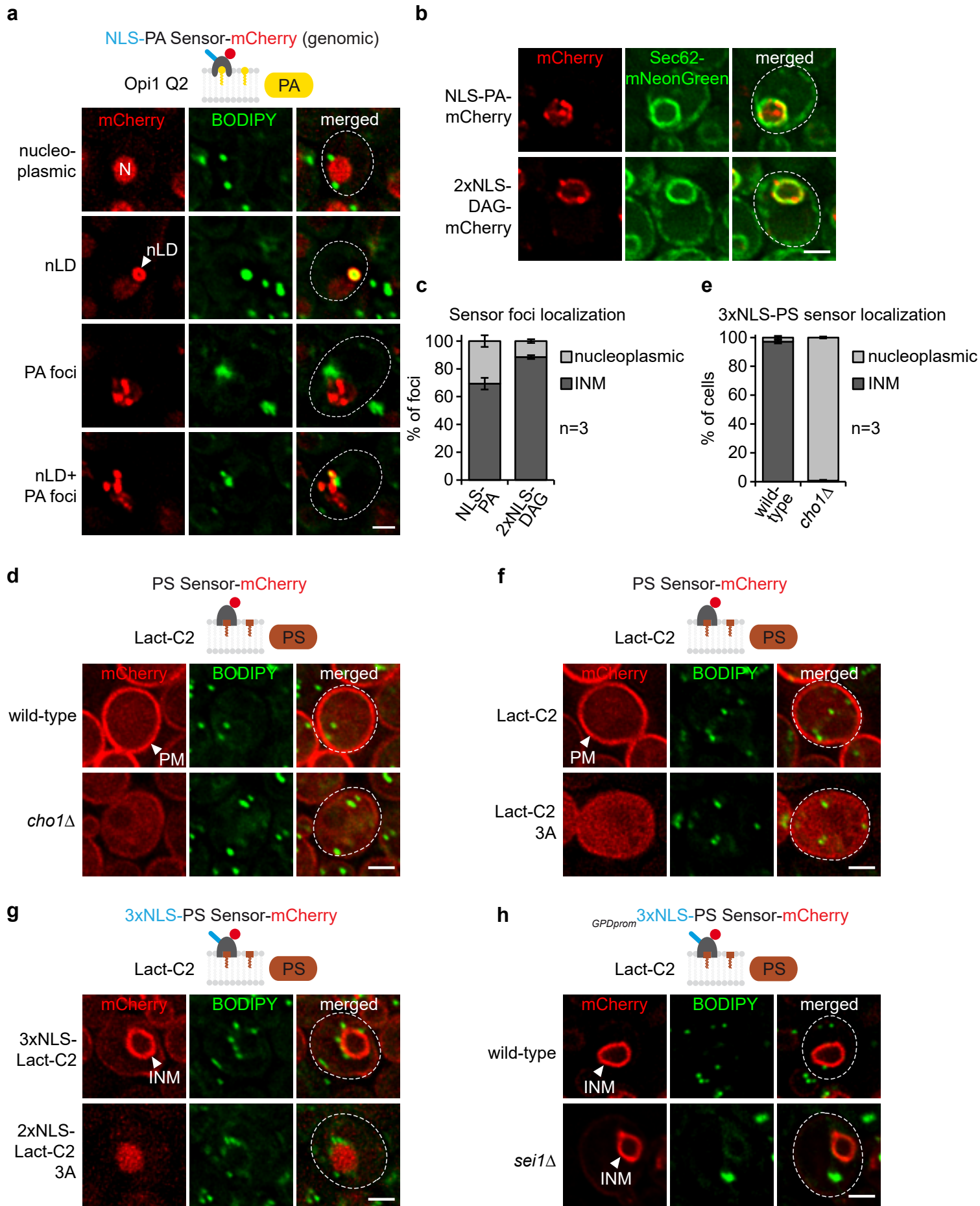


Supplementary Figure 2



**Supplementary Fig. 2 | Defects in the nuclear architecture in the absence of Sei1.**

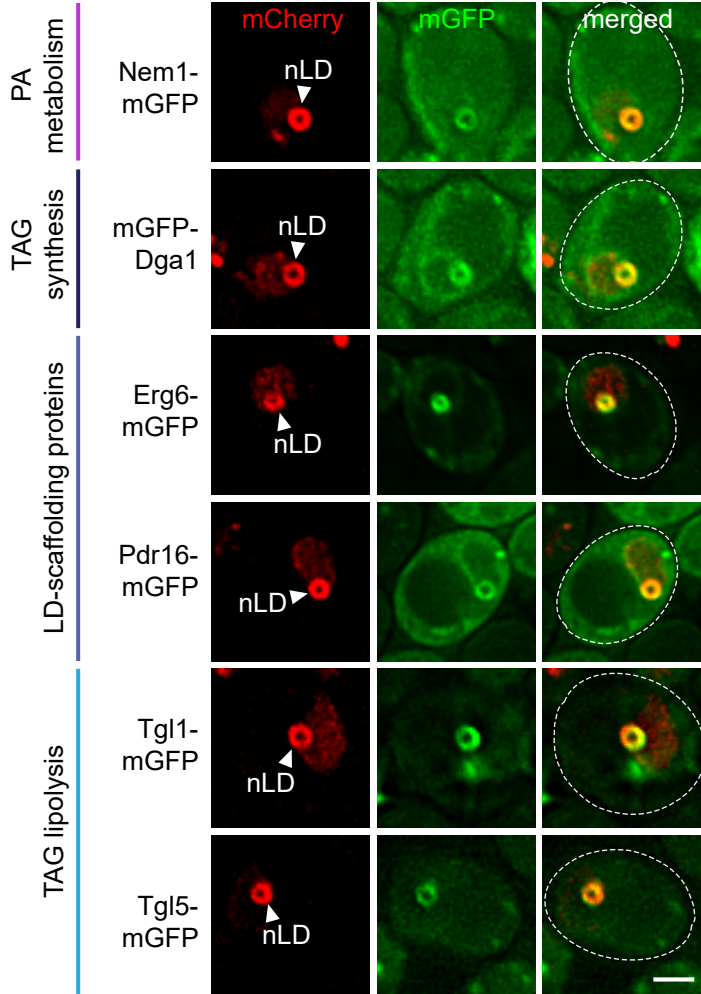
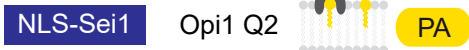
TEM analysis of representative examples of *sei1* $\Delta$  cells transformed with an empty vector and grown in SDC medium. Cells exhibit nLDs and small lipid droplet-like structures marked with a white asterisk (**a-d**), that might correspond to PA-positive foci observed by fluorescence microscopy in Fig. 2a, ectopic intranuclear membrane sheets marked with a red arrowhead (**c, e-g**) and intranuclear malformations resembling inclusions are marked with an unfilled yellow arrowhead (**h-l**). Insets show a magnified view of the marked areas. N, nucleus; NE, nuclear envelope; cLD, cytoplasmic lipid droplet; V, vacuole. Scale bar, 1  $\mu$ m; 200 nm for insets.





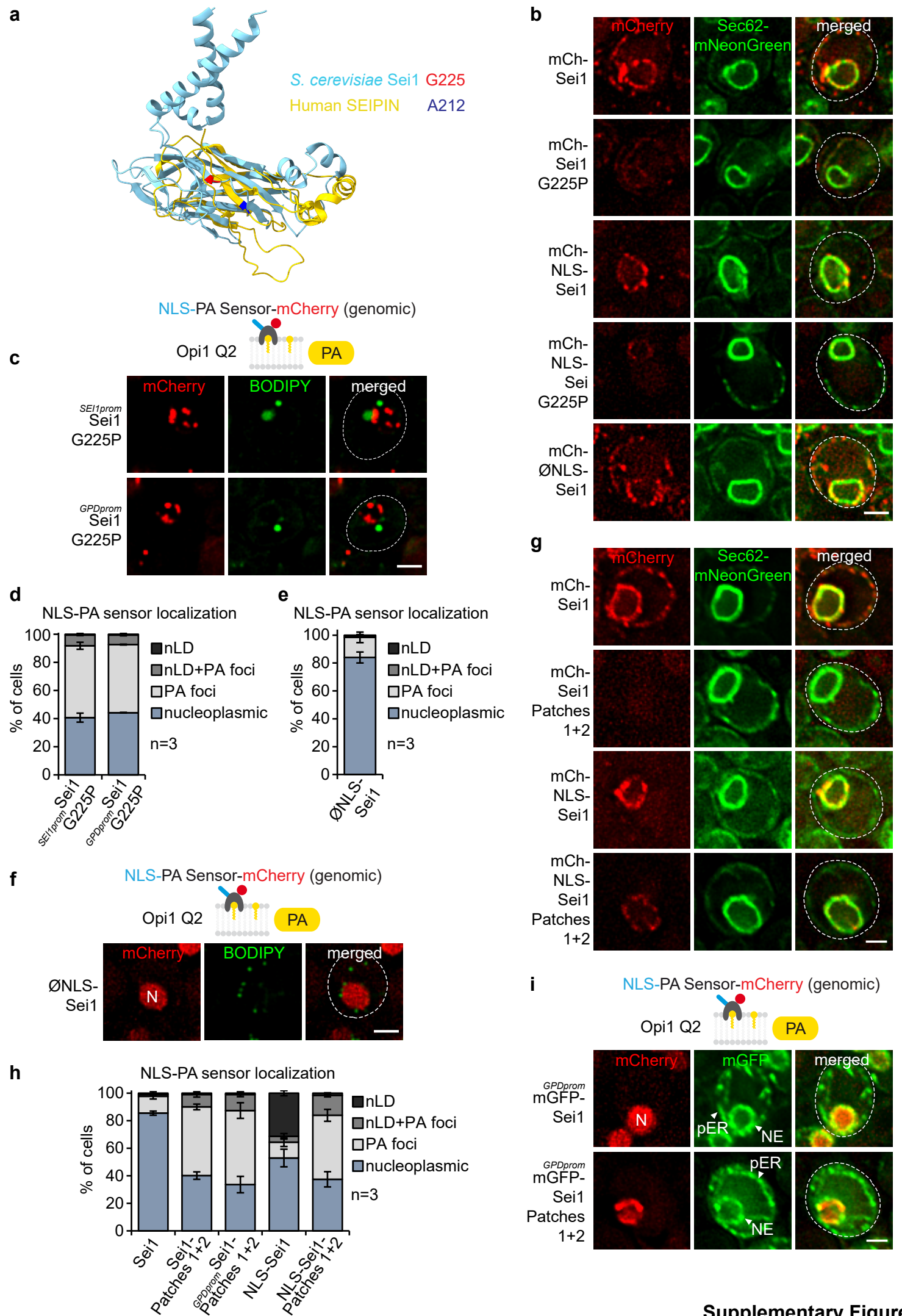
**Supplementary Fig. 3 | Mutations in Lact-C2 domain impair PS sensor binding to the INM.** **a** Exemplary images of PA sensor phenotypes in *sei1* $\Delta$  cells expressing integrated NLS-PA-mCherry sensor. BODIPY stains LDs. N, nucleus; nLD, nuclear lipid droplet. Scale bar, 2  $\mu$ m. **b** Live imaging of *sei1* $\Delta$  cells expressing plasmid-based 2xNLS-DAG-mCherry or integrated NLS-PA-mCherry sensor and plasmid-based *SEC62*-mNeonGreen. Scale bar, 2  $\mu$ m. **c** Quantification of sensor foci localization in (b). Mean value and standard deviation indicated. n, number of biological replicates. 557 foci of NLS-PA sensor and 630 foci of 2xNLS-DAG sensor were analysed. Source data are provided as a Source Data file. **d** Live imaging of wild-type or *cho1* $\Delta$  cells expressing plasmid-based PS-mCherry sensor and stained with BODIPY. PM, plasma membrane. Scale bar, 2  $\mu$ m. **e** Quantification of 3xNLS-PS-mCherry sensor localization in wild-type and *cho1* $\Delta$  cells. Mean value and standard deviation indicated. n, number of biological replicates. 297 cells for *cho1* $\Delta$  and 362 cells for wild-type analysed. Both strains were supplemented with ethanolamine and the sensor was expressed from the *GPD* promoter. Source data are provided as a Source Data file. **f** Live imaging of wild-type cells expressing plasmid-based PS-mCherry sensor or its mutant version (Lact-C2 3A) and stained with BODIPY. PM, plasma membrane. Scale bar, 2  $\mu$ m. **g** Live imaging of wild-type cells expressing plasmid-based 3xNLS-PS-mCherry sensor or its mutant version (Lact-C2 3A) and stained with BODIPY. Lact-C2 mutant fused with 3xNLS was found to have a weak fluorescence signal, making it difficult to detect. As a result, the control experiment for the Lact-C2 mutant was conducted using the 2xNLS variant. INM, inner nuclear membrane. Scale bar, 2  $\mu$ m. **h** Live imaging of wild-type or *sei1* $\Delta$  cells expressing plasmid-based 3xNLS-PS-mCherry sensor and stained with BODIPY. 3xNLS-PS-mCherry expressed from the strong *GPD* promoter. INM, inner nuclear membrane. Scale bar, 2  $\mu$ m.

**a** NLS-PA Sensor-mCherry (genomic)





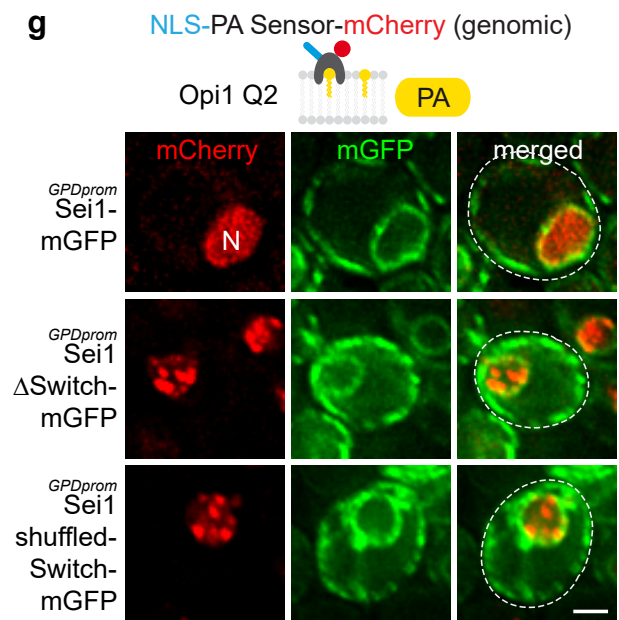
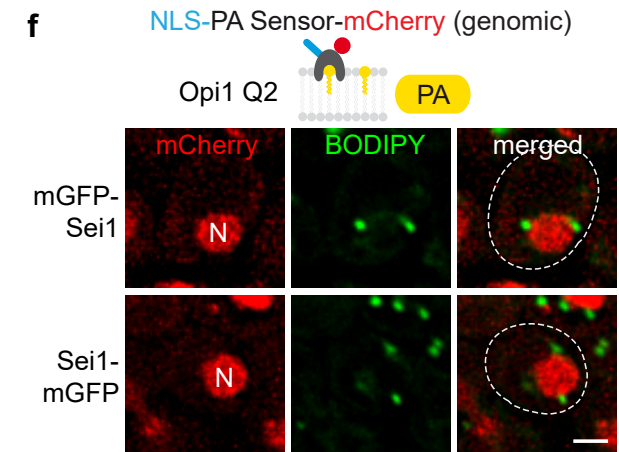
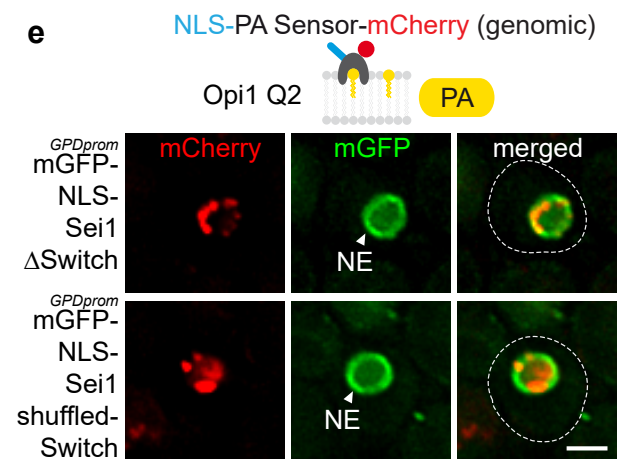
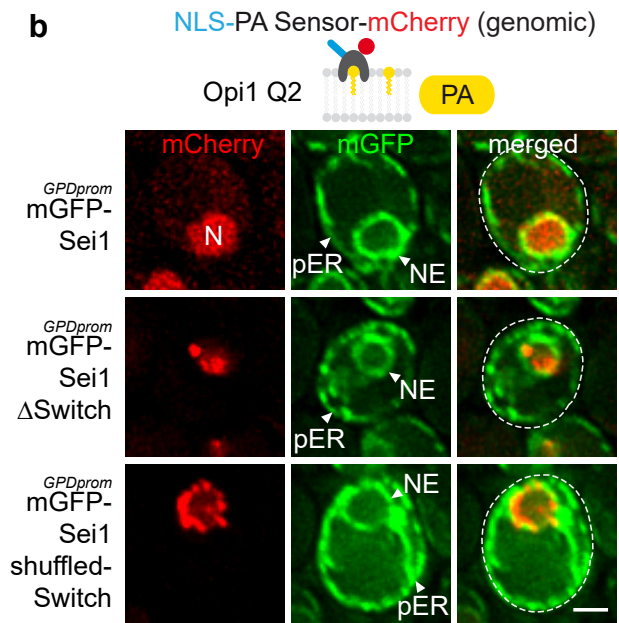
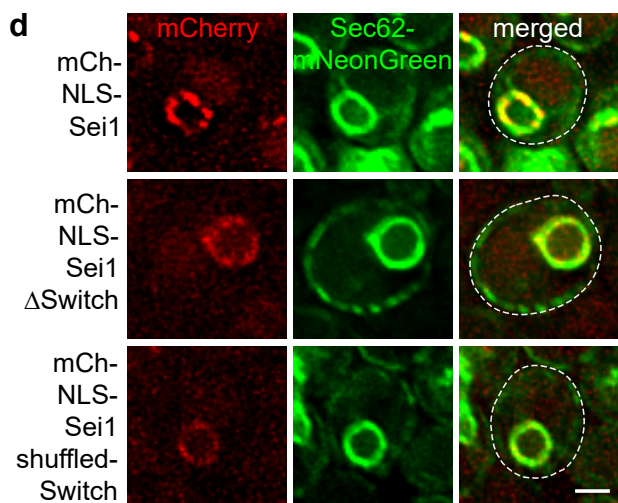
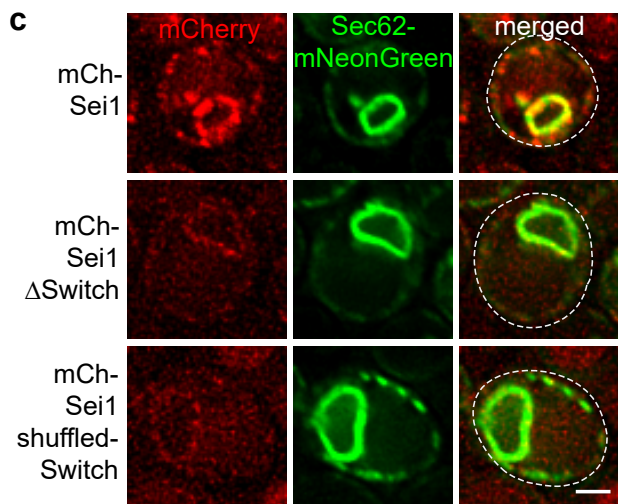
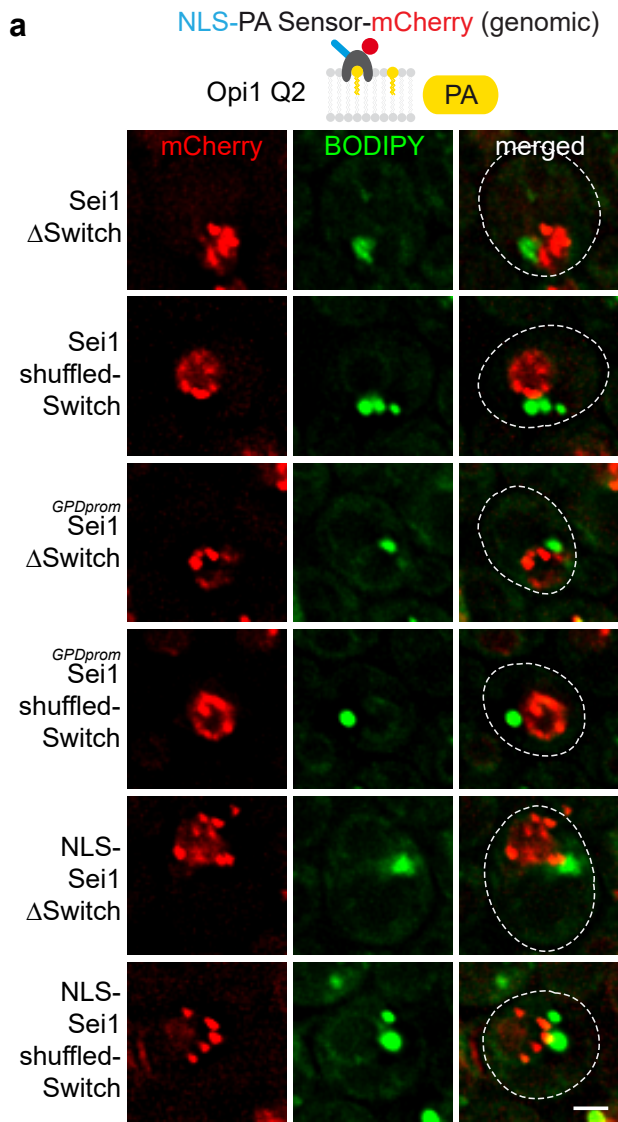
**Supplementary Fig. 4 | Inventory of nLD biogenesis factors. a** Live imaging of *sei1* $\Delta$  cells expressing plasmid-based NLS-*SEI1*, the indicated mGFP-tagged constructs expressed from their endogenous promoters and genomically integrated NLS-PA-mCherry sensor. nLD, nuclear lipid droplet. Scale bar, 2  $\mu$ m.



Supplementary Figure 5



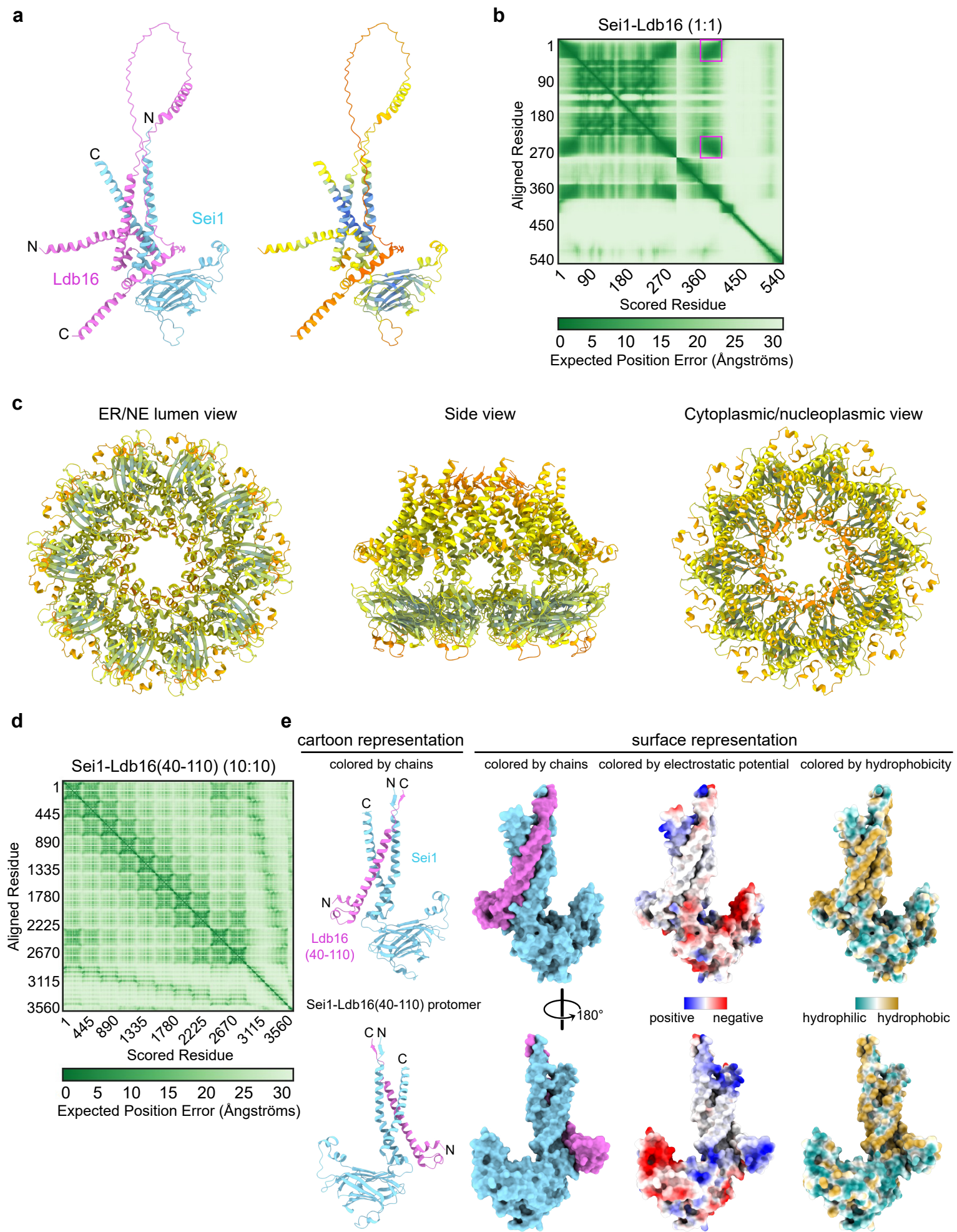
**Supplementary Fig. 5 | Expression levels of Sei1 constructs.** **a** Superposition of *S. cerevisiae* Sei1 (PDB ID: 7RSL, cyan) and human Seipin (PDB ID: 6DS5, yellow) shown in cartoon representations. Previously reported orthologous amino acid residues (yeast G225 and human A212)<sup>1</sup> are coloured in red and blue, respectively. **b** Live imaging of *sei1* $\Delta$  cells expressing plasmid-based mCh-*SEI1* constructs and an ER marker *SEC62*-mNeonGreen. NLS-Sei1 contains the nuclear localization sequence (NLS) and the linker of the INM protein Heh2, whereas the  $\emptyset$ NLS-Sei1 lacks the NLS and contains only the linker of the INM transmembrane protein Heh2 (aa138-317) attached to Sei1. Scale bar, 2  $\mu$ m. **c** Live imaging of *sei1* $\Delta$  cells expressing integrated NLS-PA-mCherry sensor and plasmid-based mGFP-*sei1* G225P constructs from the endogenous *SEI1* or a strong *GPD* promoter. BODIPY stains LDs. Scale bar, 2  $\mu$ m. **d** Quantification of NLS-PA-mCherry sensor localization in (c). Mean value and standard deviation indicated. n, number of biological replicates. 481 cells expressing *sei1* G225P from the *SEI1* promoter and 473 cells expressing *sei1* G225P from the *GPD* promoter were analysed. Source data are provided as a Source Data file. **e** Quantification of NLS-PA-mCherry sensor localization in (f). Mean value and standard deviation indicated. n, number of biological replicates. 484 cells were analysed. Source data are provided as a Source Data file. **f** Live imaging of *sei1* $\Delta$  cells expressing integrated NLS-PA-mCherry sensor and plasmid-based mGFP- $\emptyset$ NLS-*SEI1* construct.  $\emptyset$ NLS-Sei1 lacks the NLS and contains only the linker of the INM transmembrane protein Heh2 (aa138-317) attached to Sei1. BODIPY stains LDs. Scale bar, 2  $\mu$ m. **g** Live imaging of *sei1* $\Delta$  cells expressing plasmid-based mCh-*SEI1* constructs and an ER marker *SEC62*-mNeonGreen. Scale bar, 2  $\mu$ m. **h** Quantification of NLS-PA-mCherry sensor localization in (Fig. 5f). Mean value and standard deviation indicated. n, number of biological replicates. More than 440 cells analysed for each condition. Source data are provided as a Source Data file. **i** Live imaging of *sei1* $\Delta$  cells expressing integrated NLS-PA-mCherry sensor and indicated plasmid-based mGFP-*SEI1* constructs. *SEI1* constructs are expressed from the strong *GPD* promoter. NE, nuclear envelope; pER, peripheral endoplasmic reticulum. Scale bar, 2  $\mu$ m.



### Supplementary Fig. 6 | PA defects at the INM in Sei1 Switch mutants.

Conformational changes of Sei1 may facilitate the transition from a membrane-contained TAG lens to an LD bud<sup>2</sup>. Hence, we tested how mutating a previously identified switch region (see Fig. 5a) might affect INM PA. Deletion of the switch region ( $\Delta$ Switch,  $\Delta$ 51-55 and  $\Delta$ 231-239) or shuffling the amino acid sequence of the switch region (shuffled-Switch, aa46-55 PADSSNVVPL shuffled to VDPSLSAVPN and aa231-243 NFEQGLRNLMRLK to LRKNNLFLEMQRG) resulted in mutants with an abnormal PA pattern resembling a Seipin deficiency and they were unable to form nLDs upon being targeted to the INM (a). Since these mutants exhibit decreased protein expression levels (c, d) we tested whether overexpression from a strong *GPD* promoter would rescue their function. However, even when overexpressed, these mutants failed to ensure PA homeostasis and formed nLDs (a, b, e). We ensured that the position of Sei1 tagging has no impact on the outcome (f, g). Nonetheless, it is possible that these mutations might not only affect the conformational switch in the Sei1 homodecamer, but also compromise the structural integrity of Sei1. This is, because residues 51-55 are located in one of the  $\beta$ -strands within the  $\beta$ -fold of the Sei1 luminal domain (Fig. 5b). **a** Live imaging of *sei1* $\Delta$  cells expressing integrated NLS-PA-mCherry sensor and indicated plasmid-based mGFP-*SEI1* constructs from the endogenous *SEI1* or a strong *GPD* promoter. BODIPY stains LDs. Scale bar, 2  $\mu$ m. **b** Live imaging of *sei1* $\Delta$  cells expressing integrated NLS-PA-mCherry sensor and indicated plasmid-based mGFP-*SEI1* constructs from the *GPD* promoter. Scale bar, 2  $\mu$ m. **c** Live imaging of *sei1* $\Delta$  cells expressing plasmid-based mCh-*SEI1* constructs and an ER marker *SEC62*-mNeonGreen. Scale bar, 2  $\mu$ m. **d** Live imaging of *sei1* $\Delta$  cells expressing plasmid-based mCh-NLS-*SEI1* constructs and an ER marker *SEC62*-mNeonGreen. Scale bar, 2  $\mu$ m. **e** Live imaging of *sei1* $\Delta$  cells expressing integrated NLS-PA-mCherry sensor and indicated plasmid-based mGFP-NLS-*SEI1* constructs from the strong *GPD* promoter. NE, nuclear envelope. Scale bar, 2  $\mu$ m. **f** Live imaging of *sei1* $\Delta$  cells expressing integrated NLS-PA-mCherry sensor and plasmid-based *SEI1* tagged N- or C-terminally with mGFP. BODIPY stains LDs. Scale bar, 2  $\mu$ m. **g** Live imaging of *sei1* $\Delta$  cells expressing integrated NLS-PA-mCherry sensor and plasmid-based *SEI1* constructs tagged C-terminally with mGFP. *SEI1* constructs expressed from the strong *GPD* promoter. Scale bar, 2  $\mu$ m.







**Supplementary Fig. 7 | *In silico* structure of the Ldb16-Sei1 complex.** **a** Cartoon representation of AlphaFold 3 model of *S. cerevisiae* Sei1-Ldb16 heterodimer coloured by chains (left) and by per-atom confidence score (pLDDT, blue: high confidence, orange: low confidence) (right). **b** Predicted-aligned error (PAE) map of Sei1-Ldb16 heterodimer model. Note that only a single transmembrane segment of Ldb16 (violet boxes) is positioned confidently in relation to two transmembrane segments of Sei1. **c** Cartoon representation of AlphaFold 3 model of Sei1-Ldb16(40-110) 10:10 ring assembly coloured by per-atom confidence score (pLDDT, blue: high confidence, orange: low confidence). **d** Predicted-aligned error (PAE) map of Sei1-Ldb16(40-110) 10:10 ring assembly model. **e** Cartoon and surface representations of Sei1-Ldb16(40-110) protomer, coloured by either chain (left panels) or physicochemical properties (right panels: electrostatic potential and hydrophobicity).

**Supplementary Table 1. Yeast strains used in this study.**

<b>Yeast strain</b>	<b>Source</b>	<b>Identifier</b>
wild-type (BY4741), genotype: <i>MATa</i> ; <i>ura3Δ0</i> ; <i>leu2Δ0</i> ; <i>his3Δ1</i> ; <i>met15Δ0</i>	Euroscarf	Y00000
<i>sei1Δ</i> , genotype: <i>MATa</i> ; <i>ura3Δ0</i> ; <i>leu2Δ0</i> ; <i>his3Δ1</i> ; <i>met15Δ0</i> ; <i>sei1Δ::kanMX4</i>	Euroscarf	Y05313
<i>ldb16Δ</i> , genotype: <i>MATa</i> ; <i>ura3Δ0</i> ; <i>leu2Δ0</i> ; <i>his3Δ1</i> ; <i>met15Δ0</i> ; <i>ldb16Δ::kanMX4</i>	Euroscarf	Y03413
<i>sei1Δ NLS-PA-mCherry</i> , genotype: <i>MATa</i> ; <i>ura3Δ0</i> ; <i>leu2Δ0</i> ; <i>his3Δ1</i> ; <i>met15Δ0</i> ; <i>sei1Δ::kanMX4</i> ; <i>ADH1prom-NLS-PA-mCherry::HIS3</i>	3	N/A
<i>ldb16Δ NLS-PA-mCherry</i> , genotype: <i>MATa</i> ; <i>ura3Δ0</i> ; <i>leu2Δ0</i> ; <i>his3Δ1</i> ; <i>met15Δ0</i> ; <i>ldb16Δ::kanMX4</i> ; <i>ADH1prom-NLS-PA-mCherry::HIS3</i>	This study	N/A
<i>NLS-PA-mCherry</i> , genotype: <i>MATa</i> ; <i>ura3Δ0</i> ; <i>leu2Δ0</i> ; <i>his3Δ1</i> ; <i>met15Δ0</i> ; <i>ADH1prom-NLS-PA-mCherry::HIS3</i>	3	N/A
<i>sei1Δ ldb16Δ NLS-Q2-mCherry</i> , genotype: <i>MATa</i> ; <i>ura3Δ0</i> ; <i>leu2Δ0</i> ; <i>his3Δ1</i> ; <i>met15Δ0</i> ; <i>sei1Δ::kanMX4</i> , <i>ldb16Δ::natNT2</i> ; <i>ADH1prom-NLS-PA-mCherry::HIS3</i>	This study	N/A
<i>sei1Δ ldb16Δ NLS-Q2-mCherry LDB16-mGFP</i> , genotype: <i>MATa</i> ; <i>ura3Δ0</i> ; <i>leu2Δ0</i> ; <i>his3Δ1</i> ; <i>met15Δ0</i> ; <i>sei1Δ::kanMX4</i> , <i>ldb16Δ::natNT2</i> ; <i>ADH1prom-NLS-PA-mCherry::HIS3</i> ; <i>ADH1prom-LDB16-mGFP::URA3</i>	This study	N/A
<i>sei1Δ ldb16Δ NLS-Q2-mCherry ldb16 6A-mGFP</i> , genotype: <i>MATa</i> ; <i>ura3Δ0</i> ; <i>leu2Δ0</i> ; <i>his3Δ1</i> ; <i>met15Δ0</i> ; <i>sei1Δ::kanMX4</i> , <i>ldb16Δ::natNT2</i> ; <i>ADH1prom-NLS-PA-</i>	This study	N/A

<i>mCherry::HIS3; ADH1prom-ldb16 T52A S53A S55A T61A S62A T63A-mGFP::URA3</i>		
<i>NLS-Q2-mCherry ERG6-mNeonGreen</i> (query strain for the screen on YMS721 background), genotype: <i>MATa; his3Δ1; leu2Δ0; met15Δ0; ura3Δ0; can1Δ::STE2pr-SpHIS5; lyp1Δ::STE3pr-LEU2; ADH1prom-NLS-PA-mCherry::URA3; ERG6-mNeonGreen::natNT2</i>	This study	N/A
<i>ino4Δ</i> , genotype: <i>MATa; ura3Δ0; leu2Δ0; his3Δ1; met15Δ0; ino4Δ::kanMX4</i>	Euroscarf	Y06258
<i>ino2Δ</i> , genotype: <i>MATa; ura3Δ0; leu2Δ0; his3Δ1; met15Δ0; ino2Δ::kanMX4</i>	Euroscarf	Y04057
<i>opi3Δ</i> , genotype: <i>MATa; ura3Δ0; leu2Δ0; his3Δ1; met15Δ0; opi3Δ::kanMX4</i>	Euroscarf	Y02551
<i>cho2Δ</i> , genotype: <i>MATa; ura3Δ0; leu2Δ0; his3Δ1; met15Δ0; cho2Δ::kanMX4</i>	Euroscarf	Y04787
<i>cho1Δ</i> , genotype: <i>MATa; ura3Δ0; leu2Δ0; his3Δ1; met15Δ0; cho1Δ::kanMX4</i>	Euroscarf	Y07756
<i>psd1Δ</i> , genotype: <i>MATa; ura3Δ0; leu2Δ0; his3Δ1; met15Δ0; psd1Δ::kanMX4</i>	Euroscarf	Y02043
<i>med5Δ</i> , genotype: <i>MATa; ura3Δ0; leu2Δ0; his3Δ1; met15Δ0; med5Δ::kanMX4</i>	Euroscarf	Y04518
<i>cka2Δ</i> , genotype: <i>MATa; ura3Δ0; leu2Δ0; his3Δ1; met15Δ0; cka2Δ::kanMX4</i>	Euroscarf	Y01837
Yeast DAmP (Decreased Abundance by mRNA Perturbation) library	4	N/A
Yeast deletion library	5	N/A

**Supplementary Table 2. Plasmids used in this study.**

<b>Plasmid</b>	<b>Source</b>	<b>Identifier</b>
Yeast plasmids based on the pRS31X series	6	N/A
NLS-PA-mCherry (for integration): <i>pRS306-ADH1prom-NUP60(1-24)-OPI1(103-191)-mCherry</i>	This study	N/A
NLS-PA-mCherry (for integration): <i>pRS303-ADH1prom-NUP60(1-24)-OPI1(103-191)-mCherry</i>	3	N/A
NLS-PA-mCherry: <i>pRS316/pRS313-CYC1prom-NUP60(1-24)-OPI1(103-191)-mCherry</i>	7	N/A
NLS-PA-mGFP: <i>pRS316-CYC1prom-NUP60(1-24)-OPI1(103-191)-mGFP</i>	7	N/A
2xNLS-DAG-mCherry: <i>pRS313-ADH1prom-2xNUP60(1-24)-R.n. C1a+C1b-mCherry</i>	This study	N/A
3xNLS-PS-mCherry: <i>pRS313-ADH1prom/GPDprom-3xNUP60(1-24)-B.t. Lact-C2-mCherry</i>	This study	N/A
2xNLS-PS 3A-mCherry: <i>pRS313-ADH1prom-2xNUP60(1-24)-B.t. Lact-C2 W26A W33A F34A-mCherry</i>	This study	N/A
PS-mCherry: <i>pRS313-ADH1prom-B.t. Lact-C2-mCherry</i>	This study	N/A
PS 3A-mCherry: <i>pRS313-ADH1prom-B.t. Lact-C2 W26A W33A F34A-mCherry</i>	This study	N/A
Ldb16-VC: <i>pRS313-GPDprom-Ldb16-5xGS-VC</i>	This study	N/A
Nup60-VN: <i>pRS315-NUP60prom-NUP60-GS-VN</i>	7	N/A
NLS-Sei1: <i>pRS315/pRS316-SEI1prom-HEH2(93-317)-SEI1</i>	This study	N/A



mGFP-NLS-Sei1: <i>pRS315-SEI1prom-mGFP-HEH2(93-317)-SEI1</i>	3	N/A
mCherry-NLS-Sei1: <i>pRS315-SEI1prom-mCherry-HEH2(93-317)-SEI1</i>	3	N/A
NLS-PA-mCherry-VN: <i>pRS315-GPDprom-NUP60(1-24)-OPI1(103-191)-mCherry-GS-VN</i>	This study	N/A
Ldb16-mGFP: <i>pRS313-ADH1prom-Ldb16-mGFP</i>	This study	N/A
Ldb16-mGFP (for integration): <i>pRS306-ADH1prom-Ldb16-mGFP</i>	This study	N/A
Ldb16 6A-mGFP: <i>pRS313-ADH1prom-ldb16 T52A S53A S55A T61A S62A T63A-mGFP</i>	This study	N/A
Ldb16 6A-mGFP (for integration): <i>pRS306-ADH1prom-ldb16 T52A S53A S55A T61A S62A T63A-mGFP</i>	This study	N/A
<i>DGA1</i> mGFP-Dga1: <i>pRS316-DGA1prom-mGFP-Dga1</i>	This study	N/A
mGFP-Dga1: <i>pRS316-GPDprom-mGFP-Dga1</i>	This study	N/A
Pet10-mGFP: <i>pRS316-Pet10prom-Pet10-mGFP</i>	This study	N/A
Pah1-mGFP: <i>pRS316-GPDprom-Pah1-mGFP</i>	This study	N/A
<i>NEM1</i> Nem1-mGFP: <i>pRS316-NEM1prom-Nem1-mGFP</i>	This study	N/A
Nem1-mGFP: <i>pRS316/pRS315-GPDprom-Nem1-mGFP</i>	This study	N/A
mGFP-Lro1: <i>pRS316/pRS315-GPDprom-mGFP-Lro1</i>	This study	N/A
Spo7-mGFP: <i>pRS315-GPDprom-Spo7-mGFP</i>	This study	N/A
Pex30-mGFP: <i>pRS315-Tpi1prom-Pex30-mGFP</i>	This study	N/A
<i>ERG6</i> Erg6-mGFP: <i>pRS316-ERG6prom-Erg6-mGFP</i>	This study	N/A
Erg6-mGFP: <i>pRS316-GPDprom-Erg6-mGFP</i>	This study	N/A

<i>TGL1</i> Tgl1-mGFP: <i>pRS316-TGL1prom-Tgl1-mGFP</i>	This study	N/A
Tgl1-mGFP: <i>pRS316-GPDprom-Tgl1-mGFP</i>	This study	N/A
<i>TGL5</i> Tgl5-mGFP: <i>pRS316-TGL5prom-Tgl5-mGFP</i>	This study	N/A
Tgl5-mGFP: <i>pRS316-GPDprom-Tgl5-mGFP</i>	This study	N/A
Ldo45-mGFP: <i>pRS316-GPDprom-Ldo45-mGFP</i>	This study	N/A
<i>PDR16</i> Pdr16-mGFP: <i>pRS316-PDR16prom-Pdr16-mGFP</i>	This study	N/A
Pdr16-mGFP: <i>pRS316-GPDprom-Pdr16-mGFP</i>	This study	N/A
VC-Dga1: <i>pRS313-GPDprom-VC-GS-Dga1</i>	This study	N/A
Pet10-VC: <i>pRS313-ADH1prom-Pet10-5xGS-VC</i>	This study	N/A
Pah1-VC: <i>pRS313-GPDprom-Pah1-5xGS-VC</i>	This study	N/A
Nem1-VC: <i>pRS313-GPDprom-Nem1-5xGS-VC</i>	This study	N/A
VC-Lro1: <i>pRS313-GPDprom-VC-GS-Lro1</i>	This study	N/A
Spo7-VC: <i>pRS313-GPDprom-Spo7-5xGS-VC</i>	This study	N/A
Pex30-VC: <i>pRS313-TPI1prom-Pex30-5xGS-VC</i>	This study	N/A
Erg6-VC: <i>pRS313-GPDprom-Erg6-5xGS-VC</i>	This study	N/A
Tgl1-VC: <i>pRS313-GPDprom-Tgl1-5xGS-VC</i>	This study	N/A
Tgl5-VC: <i>pRS313-GPDprom-Tgl5-5xGS-VC</i>	This study	N/A
Ldo45-VC: <i>pRS313-GPDprom-Ldo45-5xGS-VC</i>	This study	N/A
Pdr16-VC: <i>pRS313-GPDprom-Pdr16-5xGS-VC</i>	This study	N/A
Sec62-mNeonGreen: <i>pRS316-SEC62prom-SEC62-5xGS-mNeonGreen</i>	3	N/A
mGFP-Sei1: <i>pRS315-SEI1prom-mGFP-SEI1</i>	3	N/A
mCherry-Sei1: <i>pRS315-SEI1prom-mCherry-SEI1</i>	3	N/A

<i>GPDprom</i> mGFP-Sei1: <i>pRS315-GPDprom-mGFP-SEI1</i>	This study	N/A
mGFP-ØNLS-Sei1: <i>pRS315-SEI1prom-mGFP-HEH2(138-317)-SEI1</i>	3	N/A
mCherry-ØNLS-Sei1: <i>pRS315-SEI1prom-mCherry-HEH2(138-317)-SEI1</i>	3	N/A
mGFP-Sei1 G225P: <i>pRS315-SEI1prom-mGFP-sei1 G225P</i>	This study	N/A
mCherry-Sei1 G225P: <i>pRS315-SEI1prom-mCherry-sei1 G225P</i>	This study	N/A
<i>GPDprom</i> mGFP-Sei1 G225P: <i>pRS315-GPDprom-mGFP-sei1 G225P</i>	This study	N/A
mGFP-NLS-Sei1 G225P: <i>pRS315-SEI1prom-mGFP-HEH(93-317)-sei1 G225P</i>	This study	N/A
mCherry-NLS-Sei1 G225P: <i>pRS315-SEI1prom-mCherry-HEH(93-317)-sei1 G225P</i>	This study	N/A
mGFP-Sei1 Patches1+2: <i>pRS315-SEI1prom-mGFP-sei1 S33A, Y37A, Y41A (Patch 1) M240G, Y248I, F255R, I259K (Patch 2)</i>	This study	N/A
mCherry-Sei1 Patches1+2: <i>pRS315-SEI1prom-mCherry-sei1 S33A, Y37A, Y41A (Patch 1) M240G, Y248I, F255R, I259K (Patch 2)</i>	This study	N/A
mGFP-NLS-Sei1 Patches1+2: <i>pRS315-SEI1prom-mGFP-HEH2(93-317)-sei1 S33A, Y37A, Y41A (Patch 1) M240G, Y248I, F255R, I259K (Patch 2)</i>	This study	N/A
mCherry-NLS-Sei1 Patches1+2: <i>pRS315-SEI1prom-mCherry-HEH2(93-317)-sei1 S33A, Y37A, Y41A (Patch 1) M240G, Y248I, F255R, I259K (Patch 2)</i>	This study	N/A
<i>GPDprom</i> mGFP-Sei1 Patches1+2: <i>pRS315-GPDprom-mGFP-sei1 S33A, Y37A, Y41A</i>	This study	N/A

(Patch 1) M240G, Y248I, F255R, I259K (Patch 2)		
mGFP-Sei1 $\Delta$ Switch: <i>pRS315-SEI1prom-mGFP-sei1<math>\Delta</math>51-55 and <math>\Delta</math>231-239</i>	This study	N/A
mCherry-Sei1 $\Delta$ Switch: <i>pRS315-SEI1prom-mCherry-sei1<math>\Delta</math>51-55 and <math>\Delta</math>231-239</i>	This study	N/A
<i>GPDprom</i> mGFP-Sei1 $\Delta$ Switch: <i>pRS315-GPDprom-mGFP-sei1<math>\Delta</math>51-55 and <math>\Delta</math>231-239</i>	This study	N/A
mGFP-NLS-Sei1 $\Delta$ Switch: <i>pRS315-SEI1prom-mGFP-HEH2(93-317)-sei1<math>\Delta</math>51-55 and <math>\Delta</math>231-239</i>	This study	N/A
mCherry-NLS-Sei1 $\Delta$ Switch: <i>pRS315-SEI1prom-mCherry-HEH2(93-317)-sei1<math>\Delta</math>51-55 and <math>\Delta</math>231-239</i>	This study	N/A
<i>GPDprom</i> mGFP-NLS-Sei1 $\Delta$ Switch: <i>pRS315-GPDprom-mGFP-HEH2(93-317)-sei1<math>\Delta</math>51-55 and <math>\Delta</math>231-239</i>	This study	N/A
mGFP-Sei1 shuffled-Switch: <i>pRS315-SEI1prom-mGFP-sei1 aa46-55 PADSSNVVPL shuffled to VDPSLSAVPN and aa231-243 NFEQGLRNLMMLRK to LRKNNLFLEMQRG</i>	This study	N/A
mCherry-Sei1 shuffled-Switch: <i>pRS315-SEI1prom-mCherry-sei1 aa46-55 PADSSNVVPL shuffled to VDPSLSAVPN and aa231-243 NFEQGLRNLMMLRK to LRKNNLFLEMQRG</i>	This study	N/A
<i>GPDprom</i> mGFP-Sei1 shuffled-Switch: <i>pRS315-GPDprom-mGFP-sei1 aa46-55 PADSSNVVPL shuffled to VDPSLSAVPN and aa231-243 NFEQGLRNLMMLRK to LRKNNLFLEMQRG</i>	This study	N/A
mGFP-NLS-Sei1 shuffled-Switch: <i>pRS315-SEI1prom-mGFP-HEH2(93-317)-sei1 aa46-55 PADSSNVVPL shuffled to VDPSLSAVPN and</i>	This study	N/A



<i>aa231-243 NFEQGLRNLMLRK to LRKNNLFLEMQRG</i>		
<i>mCherry-NLS-Sei1 shuffled-Switch: pRS315-SEI1prom-mCherry-HEH2(93-317)-sei1 aa46-55 PADSSNVVPL shuffled to VDPSLSAVPN and aa231-243 NFEQGLRNLMLRK to LRKNNLFLEMQRG</i>	This study	N/A
<i>GPDprommGFP-NLS-Sei1 shuffled-Switch: pRS315-GPDprom-mGFP-HEH2(93-317)-sei1 aa46-55 PADSSNVVPL shuffled to VDPSLSAVPN and aa231-243 NFEQGLRNLMLRK to LRKNNLFLEMQRG</i>	This study	N/A
<i>Sei1-mGFP: pRS315-SEI1prom-SEI1-mGFP</i>	This study	N/A
<i>GPDpromSei1-mGFP: pRS315-GPDprom-SEI1-mGFP</i>	This study	N/A
<i>GPDpromSei1 ΔSwitch-mGFP: pRS315-GPDprom-sei1Δ51-55 and Δ231-239-mGFP</i>	This study	N/A
<i>GPDpromSei1 shuffled-Switch-mGFP: pRS315-GPDprom-sei1 aa46-55 PADSSNVVPL shuffled to VDPSLSAVPN and aa231-243 NFEQGLRNLMLRK to LRKNNLFLEMQRG-mGFP</i>	This study	N/A
<i>pFA6a::natNT2</i>	8	N/A
<i>pFA6a-mNeonGreen::natNT2</i>	9	N/A

## References

- 1 Szymanski, K. M. *et al.* The lipodystrophy protein seipin is found at endoplasmic reticulum lipid droplet junctions and is important for droplet morphology. *Proceedings of the National Academy of Sciences of the United States of America* **104**, 20890-20895 (2007).  
<https://doi.org:10.1073/pnas.0704154104>
- 2 Arlt, H. *et al.* Seipin forms a flexible cage at lipid droplet formation sites. *Nature structural & molecular biology* **29**, 194-202 (2022).  
<https://doi.org:10.1038/s41594-021-00718-y>
- 3 Romanauska, A. & Kohler, A. Reprogrammed lipid metabolism protects inner nuclear membrane against unsaturated fat. *Developmental cell* **56**, 2562-2578 e2563 (2021). <https://doi.org:10.1016/j.devcel.2021.07.018>
- 4 Breslow, D. K. *et al.* A comprehensive strategy enabling high-resolution functional analysis of the yeast genome. *Nature methods* **5**, 711-718 (2008).  
<https://doi.org:10.1038/nmeth.1234>
- 5 Giaever, G. *et al.* Functional profiling of the *Saccharomyces cerevisiae* genome. *Nature* **418**, 387-391 (2002). <https://doi.org:10.1038/nature00935>
- 6 Sikorski, R. S. & Hieter, P. A system of shuttle vectors and yeast host strains designed for efficient manipulation of DNA in *Saccharomyces cerevisiae*. *Genetics* **122**, 19-27 (1989).
- 7 Romanauska, A. & Kohler, A. The Inner Nuclear Membrane Is a Metabolically Active Territory that Generates Nuclear Lipid Droplets. *Cell* **174**, 700-715 e718 (2018). <https://doi.org:10.1016/j.cell.2018.05.047>
- 8 Janke, C. *et al.* A versatile toolbox for PCR-based tagging of yeast genes: new fluorescent proteins, more markers and promoter substitution cassettes. *Yeast* **21**, 947-962 (2004). <https://doi.org:10.1002/yea.1142>
- 9 Romanauska, A. & Kohler, A. Lipid saturation controls nuclear envelope function. *Nature cell biology* **25**, 1290-1302 (2023).  
<https://doi.org:10.1038/s41556-023-01207-8>